Method to observe the anomaly of magnetic susceptibility in quantum spin systems

Nobutaka Aiba* and Kiyohide Nomura†
Department of Physics, Kyushu University, Fukuoka 819-0395, Japan

(Received 4 October 2019; revised 31 July 2020; accepted 9 October 2020; published 28 October 2020)

In quantum spin systems, a phase transition is studied from the perspective of magnetization curve and a magnetic susceptibility. We propose a new method for studying the anomaly of magnetic susceptibility χ that indicates a phase transition. In addition, we introduce the fourth derivative A of the lowest-energy eigenvalue per site with respect to magnetization, i.e., the second derivative of χ^{-1}. To verify the validity of this method, we apply it to an $S = 1/2XXZ$ antiferromagnetic chain. The lowest energy of the chain is calculated by numerical diagonalization. As a result, the anomalies of χ and A exist at zero magnetization. The anomaly of A is easier to observe than that of χ, indicating that the observation of A is a more efficient method of evaluating an anomaly than that of χ. The observation of A reveals an anomaly that is different from the Kosterlitz-Thouless (KT) transition. Our method is useful in analyzing critical phenomena.

DOI: 10.1103/PhysRevB.102.134435

I. INTRODUCTION

In condensed matter physics, phase transitions and their corresponding energy gaps are an important research subject. Researching these gaps is necessary for studying the behavior of quantum spin systems. Bethe showed that an $S = 1/2\ XXZ$ chain system had the characteristic of the absence of a gap [1]. Later, Haldane argued that the difference between half-spin and integer spin systems involved the gap [2].

Many researchers observed the energy gap via the magnetization curve as a function of the magnetic field. The magnetic field at zero magnetization is equal to the magnitude of the gap. However, the method of observing the gap is not appropriate for deciding whether a spin system is gapless or gapped in numerical calculation; it is difficult to distinguish a gapless system from one with a very small energy gap [3].

Hence, Sakai and Nakano [4–7] proposed a method for distinguishing a gapless from a gapped system. They introduced the magnetic susceptibility and used numerical diagonalization. They demonstrated that the susceptibility clearly shows the variation of the energy gap with changing magnetization, in comparison to the magnetization curve. Subsequently, they found the anomaly of the magnetic susceptibility. The term "anomaly" refers to a divergence in the thermodynamic limit. This anomaly usually exhibits a phase transition.

In this paper, we propose a novel method of evaluating an anomaly by investigating the magnetic susceptibility χ and the fourth derivative A of the energy with respect to magnetization. Few investigations of high-order differentials such as A have been carried out. We show that our method is appropriate for analysis of the phase transition, compared to the method using the magnetic susceptibility χ alone. The introduction of A resolves the issue of whether the high-order differential of energy diverges. As a test case, we apply this method to the $S = 1/2XXZ$ antiferromagnetic chain, which shows the ferromagnetic phase for $\Delta \leqslant -1$, Tomonaga-Luttinger (TL) phase for $-1 < \Delta \leqslant 1$, and antiferromagnetic phase for $\Delta > 1$. Here Δ denotes an anisotropic parameter associated with the z component of the XXZ antiferromagnetic chain. The lowest energy up to 26 spins of the chain is calculated by numerical diagonalization on the basis of the Lanczos algorithm. Subsequently, we analyze the anomalies of χ and A to observe the phase transition. The results demonstrate that an anomaly of χ at zero magnetization exists under $\Delta > 1$, while an anomaly of A at zero magnetization is shown for $\Delta > 1/2$. Hence, the anomaly of A is easier to observe than that of χ.

The anomaly of A at $1/2 < \Delta < 1$ is different from that of A at $\Delta = 1$, indicating a Kosterlitz-Thouless (KT) transition. It is well established that the $-1 < \Delta \leqslant 1$ region corresponds to the TL phase, in which the scaling dimensions vary continuously with the parameter Δ [8,9]. In the $\Delta > 1$ region, a Neel state appears in which the ground state is doubly degenerate with an energy gap. Under the Hamiltonian of the $U(1)$ symmetry, the change of scaling dimensions from irrelevant to relevant indicates a KT transition that corresponds to the phase transition at $\Delta = 1$ in the $S = 1/2\ XXZ$ chain. In contrast, the scaling dimensions influencing high derivatives such as A remain irrelevant for $-1 < \Delta \leqslant 1$ [10]. Thus, the onset of the anomaly of A at $\Delta = 1/2$ is different from the KT point and does not indicate the phase transition. We refer to $-1 < \Delta < 1/2$ as TL phase (I) and $1/2 < \Delta \leqslant 1$ as TL phase (II), as the TL phase is divided by the anomaly of A. The scaling dimensions influence the corrections for various quantities such as energies, susceptibility, and high derivatives [10]. Thus, the anomalies of χ and A indicate the phase transition and the energy gap.

The starting point of the anomaly of A, i.e., $\Delta = 1/2$, corresponds to $N = 2$ supersymmetry (SUSY) from correspondence between the XXZ chain and the free boson

*n.aiba@stat.phys.kyushu-u.ac.jp
†knomura@stat.phys.kyushu-u.ac.jp

model [11] and Ashkin-Teller model [12]. Moreover, the results of our computations agree with the exact solutions under $0 \leqslant \Delta < 1$. These findings indicate that the method using A is better than that using χ for analyzing critical phenomena with phase transitions.

This paper is organized as follows. In Sec. II, the calculation method of χ and A is introduced. In Sec. III, we present our numerical results for the $S = 1/2$ XXZ chain. In Sec. IV, we compare our results to available exact solutions to investigate the behavior of A. In Sec. V, we reveal that the anomaly of A is associated with conformal field theory. The correction term is discussed from the perspective of the boundary conditions and dimension. In Sec. VI, the anomaly of χ^{-1} and A is discussed in detail from the perspective of size dependence. Section VII is the conclusion.

II. METHOD: MAGNETIC SUSCEPTIBILITY χ AND FOURTH DERIVATIVE A

In this section, we introduce the physical procedure to calculate the magnetic susceptibility χ and fourth derivative A of energy as a function of magnetization. First, we define the total spin operator in the z direction as

$$\hat{S}^z_T \equiv \sum_{j=1}^{N} \hat{S}^z_j, \tag{1}$$

where $\hat{S}^z_j$ is the jth site spin operator in the z direction and N is the system size. This operator and a Hamiltonian $\hat{\mathscr{H}}$ that shows $U(1)$ symmetry commute: $[\hat{\mathscr{H}}, \hat{S}^z_T] = 0$. Therefore, the relation is obtained that

$$\hat{\mathscr{H}} |\psi\rangle = E(N, M) |\psi\rangle , \tag{2}$$

$$\hat{S}^z_T |\psi\rangle = M |\psi\rangle \ (M = 0, \pm 1, \ldots, \pm N/2), \tag{3}$$

where $E(N, M)$ is the lowest-energy eigenvalue, M is the magnetization, and $|\psi\rangle$ is the simultaneous eigenstate. The energy of $\hat{\mathscr{H}}$ per site, $\epsilon(m)$, in the thermodynamic limit is then written [13]

$$\lim_{N\to\infty} \frac{E(N, M)}{N} = \epsilon(m), \tag{4}$$

where $m = M/N$ is the magnetization per site. In finite N cases, it is shown that

$$\frac{E(N, M)}{N} = \epsilon(m) + C(N, m), \tag{5}$$

where $C(N, m)$ is a correction term of a finite size. Generally, $\epsilon(m)$ is analytic for m in the thermodynamic limit. The term "analytic" means that the function and high-order differential are continuous (our study treats the high-order differential up to the fourth derivative). $C(N, m)$ satisfies

$$\lim_{N\to\infty} C(N, m) = 0, \tag{6}$$

$$\lim_{N\to\infty} C^{(n)}(N, m) = 0 \ (n \geqslant 1), \tag{7}$$

where $C^{(n)}(N, m)$ is the nth derivative of the correction term with respect to magnetization. The correction term depends on the boundary conditions and dimension.

Next, we define the magnetic susceptibility χ and fourth derivative A in the form

$$\chi \equiv \frac{1}{\epsilon''(m)}, \tag{8}$$

$$A \equiv \frac{\partial^2}{\partial m^2}\chi^{-1} = \frac{\partial^4}{\partial m^4}\epsilon(m). \tag{9}$$

It is shown that

$$\begin{aligned}\epsilon''(N, m) &\equiv N\{E(N, M+1) - 2E(N, M) + E(N, M-1)\} \\ &= \chi^{-1} + C''(N, m) + \frac{1}{12N^2}(\epsilon^{(4)}(m) + C^{(4)}(N, m)) \\ &\quad + \mathcal{O}\left(\frac{1}{N^4}\right),\end{aligned} \tag{10}$$

$$\begin{aligned}\epsilon^{(4)}(N, m) &\equiv N^3\{E(N, M+2) - 4E(N, M+1) + 6E(N, M) \\ &\quad - 4E(N, M-1) + E(N, M-2)\} \\ &= A + C^{(4)}(N, m) + \frac{1}{6N^2}(\epsilon^{(6)}(m) + C^{(6)}(N, m)) \\ &\quad + \mathcal{O}\left(\frac{1}{N^4}\right),\end{aligned} \tag{11}$$

where $\epsilon^{(n)}(N, m)$ is the nth finite difference between energies. $\epsilon(N, m)$ is obtained directly from numerical data in finite systems. $E(N, M+1) - 2E(N, M) + E(N, M-1)$ becomes a nonzero constant at large N when finite energy gaps exist at m. Similarly, $E(N, M+2) - 4E(N, M+1) + 6E(N, M) - 4E(N, M-1) + E(N, M-2)$ becomes a nonzero constant. For example, we consider the XXZ model at $m = 0$ and $m = \pm 1/N$. For a large anisotropic limit $\Delta \gg 1$ in the Neel region, there is an energy gap at $m = 0$ and the energies are written in the form

$$E(N, M) = E(N, 0) + |M|\Delta E, \tag{12}$$

where M is the magnetization and ΔE is an energy gap for a finite system. For large N, substituting Eq. (12) into Eq. (10), we obtain

$$\epsilon''(N, m) = \begin{cases} N(2\Delta E), & (m = 0), \\ 0, & (m \neq 0). \end{cases} \tag{13}$$

Similarly, substituting Eq. (12) into Eq. (11), we obtain

$$\epsilon^{(4)}(N, m) = \begin{cases} N^3(-4\Delta E), & (m = 0), \\ N^3(2\Delta E), & (m = \pm 1/N), \\ 0, & (m \neq 0, \pm 1/N). \end{cases} \tag{14}$$

However, for a finite anisotropy, there is some interaction between magnons. Thus, the above relations are modified to the forms

$$\epsilon''(N, m) = \begin{cases} N(2\Delta E), & (m = 0), \\ \text{finite}, & (m \neq 0), \end{cases} \tag{15}$$

$$\epsilon^{(4)}(N, m) = \begin{cases} N^3(-4\Delta E), & (m = 0), \\ N^3(2\Delta E), & (m = \pm 1/N), \\ \text{finite}, & (m \neq 0, \pm 1/N). \end{cases} \tag{16}$$

This means $\epsilon^{(4)}(N, m)$ is N^2 times as large as $\epsilon''(N, m)$. This fact shows that the anomaly of A appears stronger than that

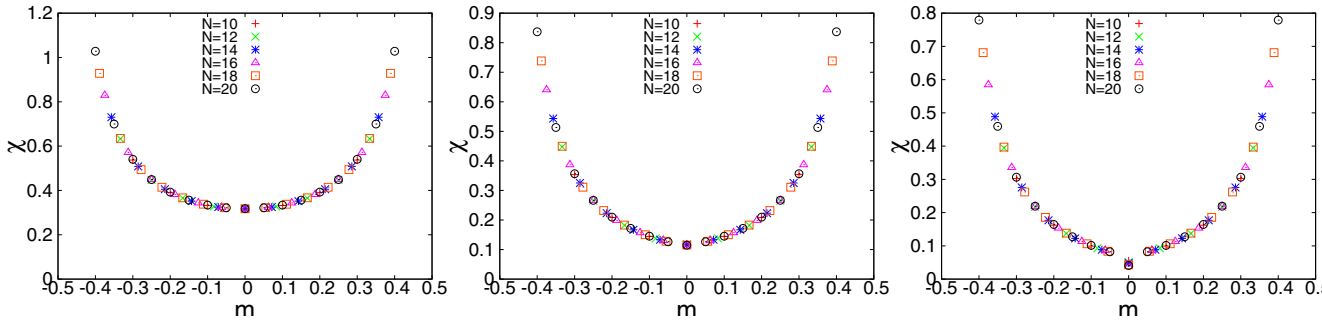

(a) $\Delta = 0$ (b) $\Delta = 1$ (c) $\Delta = 2$

FIG. 1. Magnetization dependence of the magnetic susceptibility χ of the $S = 1/2$ XXZ antiferromagnetic chain for several system sizes N: 10, 12, 14, 16, 18, and 20. Panel (c) shows that χ has a sharp cusp at zero magnetization. However, panel (c) does not exhibit an anomaly because the size dependence is small. Thus, χ does not have an anomaly.

of χ^{-1} in the thermodynamic limit. Thus, we introduce A for observing an anomaly.

Finally, we consider the case in which $\epsilon(m)$ is not analytic. $\epsilon(m)$ is not analytic for m when $\epsilon''(N, m)$ or $\epsilon^{(4)}(N, m)$ diverges. In the thermodynamic limit, it is given by

$$\begin{cases} \lim_{N\to\infty} \epsilon''(N, m) = \epsilon''(m) \\ \qquad\qquad \Rightarrow \epsilon(m) \text{ is analytic}, & (17) \\ \lim_{N\to\infty} \epsilon''(N, m) = \pm\infty \\ \qquad\qquad \Rightarrow \epsilon(m) \text{ is not analytic}. & (18) \end{cases}$$

The same holds for $\epsilon^{(4)}(N, m)$. The divergence of $\epsilon''(N, m)$ and $\epsilon^{(4)}(N, m)$ is equivalent to the fact that χ^{-1} and A diverge.

III. NUMERICAL RESULTS

We calculate the lowest-energy eigenvalue $E(N, M)$ to derive the magnetic susceptibility χ and the fourth derivative A, using numerical diagonalization by TITPACK Version 2 [14] and $H\phi$ [15]. As an example, we treat an $S = 1/2$ XXZ antiferromagnetic spin chain

$$\mathcal{H} = J \sum_{j=1}^{N} \left(\hat{S}_j^x \hat{S}_{j+1}^x + \hat{S}_j^y \hat{S}_{j+1}^y + \Delta \hat{S}_j^z \hat{S}_{j+1}^z \right), \qquad (19)$$

where $\hat{S}_j^x, \hat{S}_j^y, \hat{S}_j^z$ is the jth site spin operator in the x, y, z direction. Δ is an anisotropic parameter that takes a 0.1 increment of values from 0 to 2. The phase of the chain is changed by Δ, which shows the ferromagnetic phase for $\Delta \leqslant -1$, the Tommonaga-Luttinger phase for $-1 < \Delta \leqslant 1$, and antiferromagnetic phase for $\Delta > 1$. N is even from 10 to 26. We then give an exchange interaction $J = 1$. The boundary condition of the model is periodic:

$$\hat{S}_{N+1} = \hat{S}_1. \qquad (20)$$

In this section, we present our numerical data for $\Delta = 0, 1, 2$ with several sizes from 10 to 20.

A. Magnetic susceptibility χ and χ^{-1}

First, we show the magnetization dependence of χ in Fig. 1. Figures 1(a) and 1(b) show smooth curves. Figure 1(c) only shows a sharp cusp at zero magnetization. However, this cusp does not indicate an anomaly, as an anomaly must satisfy the following conditions: (1) χ, χ^{-1}, and A have a cusp and (2) the size dependence of the cusp is large in the thermodynamic limit. Thus, Fig. 1(c) does not show the anomaly as the size dependence is small. Similarly, neither Fig. 1(a) nor Fig. 1(b) show the anomaly. The results demonstrate that the anomaly of χ is not shown.

Next, the magnetization dependence of χ^{-1} is shown in Fig. 2. Figure 2(a) does not show an anomaly because the graph does not have a cusp. Figures 2(b) and 2(c) have sharp cusps at zero magnetization, compared to Fig. 1. Thus, it is clearer to observe the cusp of χ^{-1} than of χ. However, Fig. 2(b) does not show an anomaly as the size dependence is small at zero magnetization. In contrast, Fig. 2(c) demonstrates the possibility of showing an anomaly because the size dependence is large. The results indicate a possibility that χ^{-1} shows an anomaly for $\Delta > 1$ in the thermodynamic limit. The details are discussed in a later section.

B. Fourth derivative A

We show the magnetization dependence of A in Fig. 3, which indicates that A decreases as the magnetization approaches zero for $0 \leqslant \Delta \leqslant 1$. Figure 3(a) does not show an anomaly as the graph does not have a cusp. Figures 3(b) and 3(c) have sharp cusps at zero magnetization in comparison to Fig. 2. Furthermore, these graphs show the possibility that A at zero magnetization indicates an anomaly as its size dependence is large. This shows that it is easier to observe the possibility that an anomaly exists for A than for χ^{-1}. The difference between the graphs is the behavior of A at $m = \pm 1/N$. Figure 3(b) demonstrates that at $m = \pm 1/N$, A exhibits negative values. Although A in Fig. 3(b) appears to be discontinuous near $m = 0.1$, this behavior is superficial. In fact, Fig. 4 shows that near $m = 0.1$, A is continuous for three system sizes: 10, 14, and 20. Thus, A near $m = 0.1$ is continuous for $\Delta = 1$. In contrast, Fig. 3(c) demonstrates that A at $m = \pm 1/N$ shows large positive values, in contrast to the large negative value of A at zero magnetization.

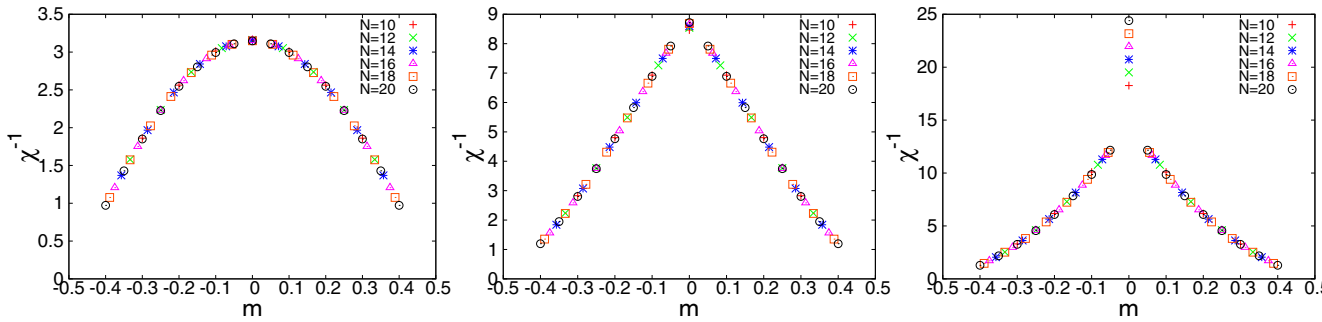

(a) $\Delta = 0$ (b) $\Delta = 1$ (c) $\Delta = 2$

FIG. 2. Magnetization dependence of the inverse of the magnetic susceptibility χ^{-1} of the $S = 1/2$ XXZ antiferromagnetic chain for several system sizes N: 10, 12, 14, 16, 18, and 20. Panel (b) demonstrates that χ^{-1} shows a cusp and a low size dependence at zero magnetization. Panel (c) demonstrates that χ^{-1} shows a sharp cusp of large positive values and high size dependence at zero magnetization, compared to panel (b). Therefore, it is easier to observe the cusp of χ^{-1} than that of χ in Fig. 1. Moreover, it is possible for χ^{-1} to show an anomaly for $\Delta > 1$ owing to its high size dependence at zero magnetization.

The behavior of A indicates the possibility of showing an anomaly as its size dependence is large. This is explained by Eq. (16). However, we do not understand how the behavior of A for $\Delta < 1$ changes in the thermodynamic limit. These details are discussed in a later section.

IV. COMPARISON TO EXACT SOLUTIONS

In this section, we compare our numerical data to exact solutions [16–20] to investigate the behavior of A. The behavior of χ is well established for all Δ. However, the behavior of A has not previously been studied. The reliability of the data of A increases when the data of χ agree with exact solutions. This leads to an investigation of the behavior of A.

A. Comparison to magnetic susceptibility near saturation magnetization

For the spin S antiferromagnetic chain, the inverse of magnetic susceptibility χ^{-1} is proportional to a magnetization $S - m$ near the saturation magnetization [21]. In our case, it is shown that

$$\chi^{-1} \propto 1/2 - m. \tag{21}$$

We investigate whether our numerical data are consistent with Eq. (21). Figure 5 shows a magnetization dependence of χ^{-1} for $\Delta = 1$ with a fitting function f that is described by Eq. (21). The fitting is performed under $0.3 \leqslant |m| \leqslant 0.4$. The graph demonstrates a linear relation between χ^{-1} and m near $m = 1/2$ because f is consistent with our data. However, the relation is not applied to the points where f is not consistent with our data. Thus, our data of χ are reliable, and the reliability of our data of A increases.

B. Comparison to Bethe-ansatz solution

The Bethe ansatz is an exact method applied in a wide range of fields, such as quantum field theory and statistical mechanics. We compare our numerical data to exact solutions. The Zeeman energy is given by

$$\hat{\mathscr{H}}_z = h \sum_{j=1}^{N} \hat{S}_j^z. \tag{22}$$

$\hat{\mathscr{H}}_z$ and the Hamiltonian in Eq. (19) commute. h is a magnetic field.

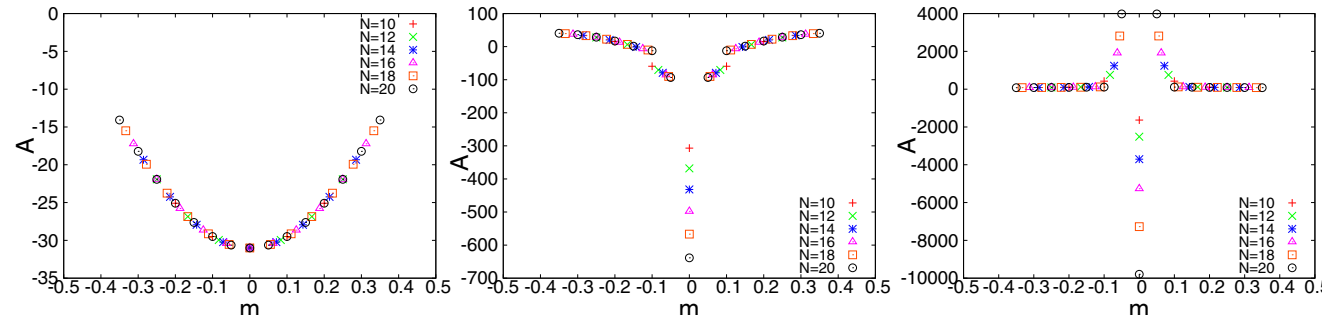

(a) $\Delta = 0$ (b) $\Delta = 1$ (c) $\Delta = 2$

FIG. 3. Magnetization dependence of the fourth derivative A of the $S = 1/2$ XXZ antiferromagnetic chain for several system sizes N: 10, 12, 14, 16, 18, and 20. Both panels (b) and (c) demonstrate that A shows a sharp cusp of large negative values and a high size dependence at zero magnetization. Furthermore, panel (c) shows that A has large positive values as the magnetization approaches zero. Therefore, it is possible for A to show an anomaly for $\Delta \geqslant 1$ owing to its high size dependence at zero magnetization.

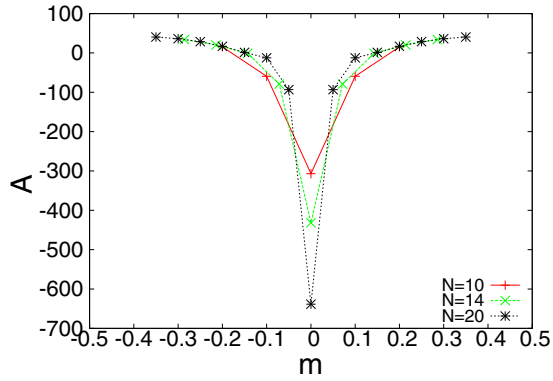

FIG. 4. Magnetization dependence of the fourth derivative A for $\Delta = 1$ for three system sizes: 10, 14, and 20. The A values form a continuous curve, in contrast with Fig. 3(b).

1. Case of χ^{-1} for $0 < \Delta \leqslant 1$

First, under $0 < \Delta < 1$, the exact solution of χ is given by [9]

$$\chi = \frac{4\gamma}{\pi(\pi-\gamma)\sin\gamma}\left\{1 + \mathcal{O}(h^2) + \mathcal{O}\left(h^{\frac{4\gamma}{\pi-\gamma}}\right)\right\}, \tag{23}$$

$$\gamma = \arccos\Delta. \tag{24}$$

We then rewrite Eq. (23) as a function of m as it is difficult to compare our numerical data with Eq. (23):

$$\chi = \frac{4\gamma}{\pi(\pi-\gamma)\sin\gamma} + c_1 m^2 + c_2|m|^{\frac{4\gamma}{\pi-\gamma}}, \tag{25}$$

$$h = \frac{4\gamma}{\pi(\pi-\gamma)\sin\gamma}m,$$

where c_1 and c_2 are constants. We perform the fitting with Eq. (25) under $0 < |m| \leqslant 0.1$. The result of this fitting is shown in Fig. 6(a). Figure 6(a) indicates that our data are consistent with exact solutions near zero magnetization. Therefore, this consistency increases the reliability of our numerical data of χ for $0 < \Delta < 1$.

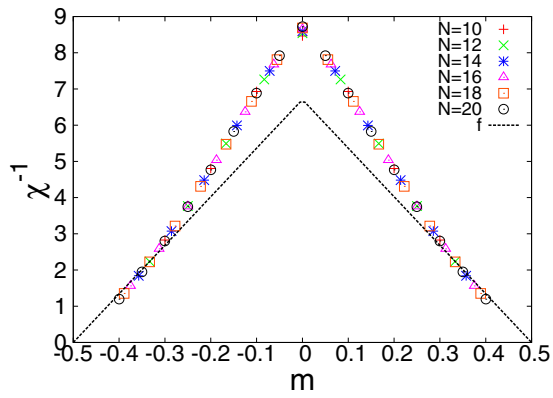

FIG. 5. Magnetization dependence of the inverse of the magnetic susceptibility χ^{-1} for $\Delta = 1$. f is the fitting function expressed by Eq. (21). Our numerical data are consistent with f near saturation magnetization.

Next, we explain the exact solution of χ for $\Delta = 1$. In this case, although it appears that $h^{\frac{4\gamma}{\pi-\gamma}} = h^0$ from Eq. (23), there remains a possibility of logarithmic behavior from the solutions of a Hubbard model [22]. The Hubbard model is regarded as an isotropic Heisenberg model with an infinite Coulomb repulsion. Thus, using the exact solution of the Hubbard model, that of χ is given by [22]

$$\frac{\chi}{\chi_0} = 1 + \frac{1}{2}\frac{1}{\ln\frac{h_c}{h}\gamma_c} - \frac{1}{4}\frac{\ln\ln\frac{h_c}{h}\gamma_c}{\left(\ln\frac{h_c}{h}\gamma_c\right)^2} + \text{h.o.}, \tag{26}$$

$$h_c = 4\sin^2\left(\frac{\pi}{2}n\right), \quad \gamma_c = \frac{\pi}{2}\sqrt{\frac{2\pi}{e}}, \tag{27}$$

where χ_0, n, and h.o. are the magnetic susceptibility at zero magnetization, a filling that denotes electron density, and high-order terms, respectively. For an isotropic Heisenberg model, $n = 1$ and $\chi_0 = 1/\pi^2$ [23,24]. Similarly, we rewrite Eq. (26) as a function of m for the Heisenberg model

$$\chi = \frac{1}{\pi^2} + \frac{1}{2\pi^2}\frac{1}{\ln\frac{2\pi\sqrt{\frac{2\pi}{e}}}{d_0 m}} - \frac{1}{4\pi^2}\frac{\ln\ln\frac{2\pi\sqrt{\frac{2\pi}{e}}}{d_0 m}}{\left(\ln\frac{2\pi\sqrt{\frac{2\pi}{e}}}{d_0 m}\right)^2},$$

$$h = d_0 m, \tag{28}$$

where d_0 is a constant. We perform the fitting with Eq. (28) under $0 \leqslant |m| \leqslant 0.1$. The result is shown in Fig. 6(b). Figure 6(b) indicates that our data are consistent with exact solutions near zero magnetization. Thus, our data are consistent with exact solutions in $0 < \Delta \leqslant 1$. This indicates that the reliability of the data of A increases with that of χ. However, for $\Delta = 1$ the magnetic susceptibility shows an infinite slope when m approaches zero from Griffiths's theory. The cause of the differences between the theoretical and calculated results is a finite-size effect.

2. Case of A

The exact solutions of A have not been investigated. However, C. N. Yang and C. P. Yang discussed [8,25]

$$\lim_{m\to 0+} A = \begin{cases} \text{finite} & (-1 < \Delta < 1/2) \quad (29) \\ \text{infinite} & (1/2 < \Delta < 1). \quad (30) \end{cases}$$

The numerical data of A are shown in Fig. 7. Figure 7(a) indicates that A becomes finite as m approaches zero because its size dependence is small. In contrast, Fig. 7(b) indicates that A appears to become infinite as m approaches zero from of its large size dependence. Thus, our data are explained by the tendency of the exact solutions. $\Delta = 1/2$ corresponds to $N = 2$ supersymmetry (SUSY) in a conformal field theory [11]. Details of this are discussed in a later section.

V. ANOMALY AND CORRECTION TERM ASSOCIATED WITH CONFORMAL FIELD THEORY

In this section, we describe the relationship between the anomaly of A and a conformal field theory (CFT). In addition, the correction term obtained from the CFT is discussed.

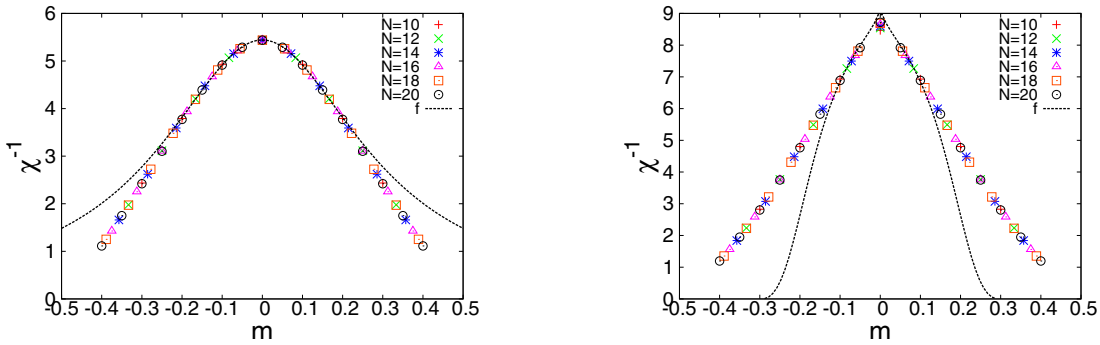

(a) $\Delta = 1/2$ (b) $\Delta = 1$

FIG. 6. Magnetization dependence of the inverse of the magnetic susceptibility χ^{-1} with a fitting function f. Panel (a) f is expressed by the inverse of Eq. (25). Panel (b) f is expressed by the inverse of Eq. (28). Our numerical data are consistent with f under $0 < |m| \leqslant 0.1$.

A. Anomaly at $\Delta = 1/2$

We demonstrate that the $\Delta = 1/2$ point corresponds to the $N = 2$ SUSY in the CFT. We apply the CFT to the $S = 1/2$ XXZ chain. The anisotropic parameter of the chain Δ is related to the scaling dimension x_T, which is associated with the critical exponent [26]. It is shown for $-1 < \Delta \leqslant 1$ that [27,28]

$$x_T(k=0) = \frac{2\pi}{\arccos(-\Delta)}, \tag{31}$$

where k is the wave number of the spin state that is a parameter obtained from translational symmetry. We focus on the scaling dimension with the wave number $k = 0$ and zero magnetization, as it is compatible with the symmetry of the Hamiltonian. For $\Delta = 1/2$, from Eq. (31), $x_T(k=0) = 3$. The scaling dimensions $x_T(k=0) > 2$ have irrelevant characteristics [26]. Thus, $x_T(k=0) = 3$ shows the irrelevant characteristics. S. K. Yang [12] demonstrated that $x_T(k=0) = 3$ corresponds to $N = 2$ SUSY from the correspondence between the XXZ chain and Ashkin-Teller model. Later, Ginsparg [11] showed the same correspondence from the relation between the XXZ chain and free boson model. Therefore, these discussions show that $\Delta = 1/2$ corresponds to $N = 2$ SUSY.

B. Anomaly and scaling dimensions

We show that the anomaly of A is influenced by scaling dimensions in the CFT. In the CFT, the energy gap ΔE for a finite system size N is given by [29]

$$\Delta E = \frac{2\pi v}{N}\left\{x + C_1\left(\frac{1}{N}\right)^{x_T-2} + C_2\left(\frac{1}{N}\right)^{2(x_T-2)}\right\}, \tag{32}$$

where x is a scaling dimension that is different from x_T, C_1 and C_2 are constants, and v is the velocity of the spin wave. For a sine-Gordon model that corresponds to the XXZ chain, $C_1 = 0$, $x_T > 2$ [30], and $C_2 < 0$ [27]. First, we consider $\epsilon^{(4)}(N, m)$ at $x_T > 2$. Next, considering $1/N \propto m$, Eq. (32) is written as

$$\Delta E = \frac{2\pi v}{N}\{x + C_2 m^{2(x_T-2)}\}. \tag{33}$$

Substituting Eq. (33) into Eq. (10), the second differentials are written by

$$\epsilon^{(2)}(N, m) = 4\pi v\{x + C_2|m|^{2(x_T-2)}\}, \tag{34}$$

where m is replaced by $|m|$ as the system has the spin reversal symmetry $m \to -m$. This equation is consistent with the exact solution of Eq. (25). The fourth differential of magnetization with respect to energy is then written in the form

$$\epsilon^{(4)}(N, m) = 4\pi v C_2(2x_T - 4)(2x_T - 5)|m|^{2(x_T-3)}. \tag{35}$$

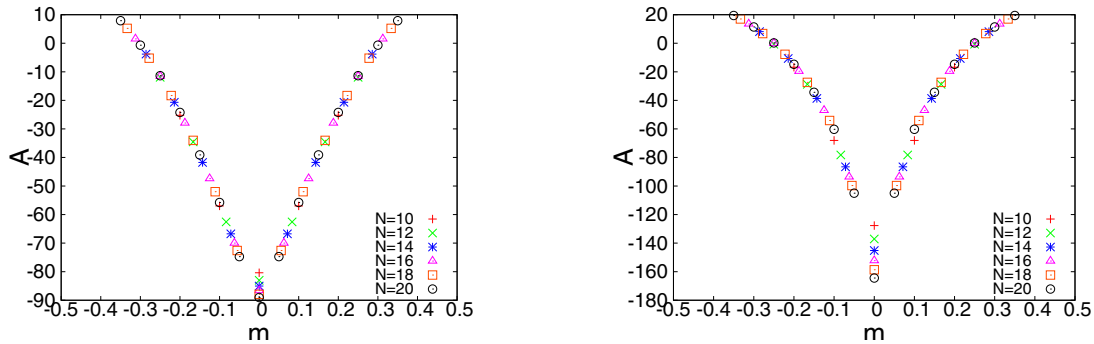

(a) $\Delta = 0.4$ (b) $\Delta = 0.6$

FIG. 7. Magnetization dependence of the fourth derivative A near $\Delta = 1/2$. Our numerical data are consistent with Eqs. (29) and (31).

$\epsilon^{(4)}(N,m)$ diverges for $2 < x_T < 3$, i.e., $1/2 < \Delta < 1$ in the thermodynamic limit. $\epsilon^{(4)}(N,m) = 0$ at $x_T = 5/2$ is a subject of future works as few investigations have been carried out. In addition, we focus on the size dependence of $\epsilon^{(4)}(N, m = 0)$. Considering the Gaussian model [27,31], we extend Eq. (33) in the form

$$\begin{aligned} &E(N,M) - 2E(N,0) + E(N,-M) \\ &\quad = E(N,M) - E(N,0) - (E(N,-M) - E(N,0)) \\ &\quad = \frac{4\pi v|M|^2}{N}\left\{x + C_2\left|\frac{M}{N}\right|^{2(x_T-2)}\right\}, \end{aligned} \tag{36}$$

where $|M| \ll N$. Although few investigations into the extension of Eq. (33) have been carried out, with respect to $|M/N|^{2(x_T-2)}$, we consider that the average distance between quasiparticles is $|N/M|$, which is renormalized by x_T. The relation is applied for the fourth differential in Eq. (11) in the form

$$\begin{aligned} \epsilon^{(4)}(N, m = 0) &= N^3\{E(N,2) - 2E(N,0) + E(N,-2) \\ &\quad - 4(E(N,1) - 2E(N,0) + E[N,-1)]\} \\ &= 16\pi v C_2(2^{2(x_T-2)} - 1)N^{6-2x_T}, \end{aligned} \tag{37}$$

where the coefficient $16\pi v C_2(2^{2(x_T-2)} - 1)$ has a negative value for $C_2 < 0$ and $x_T > 2$. Thus, $\epsilon^{(4)}(N, m = 0)$ diverges for $2 < x_T < 3$ in the thermodynamic limit.

Next, we explain $\epsilon^{(4)}(N,m)$ at $x_T = 2$, i.e., $\Delta = 1$. The energy gap ΔE is written as [19]

$$\Delta E = \frac{2\pi v}{N}\frac{1}{2}\left(1 - \frac{1}{2}\frac{1}{\ln\frac{N}{N_0}} + \frac{1}{4}\frac{\ln\left(\ln\frac{N}{N_0}\right)}{\left(\ln\frac{N}{N_0}\right)^2}\right), \tag{38}$$

where N_0 is a nonuniversal renormalization constant. Under $1/N \propto m$, substituting Eq. (38) into Eq. (10), we obtain

$$\epsilon^{(2)}(N,m) = 2\pi v\left(1 - \frac{1}{2}\frac{1}{\ln\frac{m_0}{m}} + \frac{1}{4}\frac{\ln\left(\ln\frac{m_0}{m}\right)}{\left(\ln\frac{m_0}{m}\right)^2}\right), \tag{39}$$

where m_0 is a constant that corresponds to $1/N_0$. Hence, the fourth differentials are shown by

$$\begin{aligned} \epsilon^{(4)}(N,m) = \pi v\left(m\ln\frac{m_0}{m}\right)^{-2}\Bigg\{1 - \frac{\ln\left[\ln\frac{m_0}{m}\right] + 3/2}{\ln\frac{m_0}{m}} \\ + \mathcal{O}\left[\left(\ln\frac{m_0}{m}\right)^{-2}\right]\Bigg\}. \end{aligned} \tag{40}$$

Thus, $\epsilon^{(4)}(N,m)$ diverges in the thermodynamic limit. Furthermore, we discuss the size dependence of $\epsilon^{(4)}(N, m = 0)$. We use Eq. (38) in the same procedure as for Eq. (36) and obtain

$$\begin{aligned} &E(N,M) - 2E(N,0) + E(N,-M) \\ &\quad = \frac{2\pi v}{N}|M|^2\left(1 - \frac{1}{2}\frac{1}{\ln\frac{N}{N_0|M|}} + \frac{1}{4}\frac{\ln\left(\ln\frac{N}{N_0|M|}\right)}{\left(\ln\frac{N}{N_0|M|}\right)^2}\right). \end{aligned} \tag{41}$$

Using this relation, the fourth differentials are expressed by

$$\epsilon^{(4)}(N, m = 0) = -4\pi v N^2\left(\ln\frac{N}{N_0}\right)^{-2}\ln 2\left\{1 - \frac{\ln\left(\ln\frac{N}{N_0}\right) - \ln 2 - 1/2}{\ln\frac{N}{N_0}} + \mathcal{O}\left[\left(\ln\frac{N}{N_0}\right)^{-2}\right]\right\}. \tag{42}$$

Therefore, $\epsilon^{(4)}(N, m = 0)$ diverges in the thermodynamic limit.

These facts indicate that the scaling dimension x_T influences the energy gap, magnetic susceptibility, and fourth derivative for a finite magnetization. The anomalies of χ and A are subject to the change in scaling dimension that is related to phase transition.

C. Scaling dimension and phase transition

We explain that the scaling dimension x_T is related to phase transition. To demonstrate this, Fig. 8 indicates the Δ dependence of the fourth derivative A at zero magnetization. It appears that A diverges for $\Delta > 1/2$ as the size dependence is large. This is as expected by C. N. Yang and C. P. Yang [8,25]. However, the anomaly of A at $\Delta = 1/2$ is different from that at $\Delta = 1$ from the perspective of the scaling dimension x_T. Generally, the $-1 < \Delta \leqslant 1$ region corresponds to the TL phase, which is controlled by the scaling dimension x_T subject to the parameter Δ [8,9]. For $\Delta = 1$, the anomaly of A represents the phase transition corresponding to the KT transition when the scaling dimension x_T changes from irrelevant to relevant for $U(1)$ symmetry. In contrast, for $\Delta = 1/2$, the anomaly of A does not represent the phase transition as the scaling dimension x_T is irrelevant in the $-1 < \Delta \leqslant 1$ region [10]. Similarly, the anomaly of A for $\Delta = 2$ does not represent the phase transition as the scaling dimension x_T is relevant in $\Delta > 1$. Therefore, the phase transition is controlled by the scaling dimension x_T. These facts show that the anomalies of χ and A represent the phase transition through the scaling dimension x_T. In addition to this, we name $-1 < \Delta < 1/2$ TL phase (I) and $1/2 < \Delta \leqslant 1$ TL phase (II) based on the behavior of A for $\Delta > 1/2$.

D. Correction term and boundary conditions

The correction term of Eq. (5) changes in relation to boundary conditions and dimension. First, we discuss $C(N,m)$ in one-dimensional systems. Without anomaly, $C(N,m)$ in a periodic boundary condition is written in the CFT as [32–34]

$$C(N,m) = -\frac{\pi v(m)}{6N^2}, \tag{43}$$

where $v(m)$ is the velocity of the spin wave and a smooth function for m. Thus, $\epsilon''(N,m)$ and $\epsilon^{(4)}(N,m)$ in Eqs. (10) and (11) converges to $1/N^2$ order, which agrees with our numerical results. In contrast, the correction term for an open

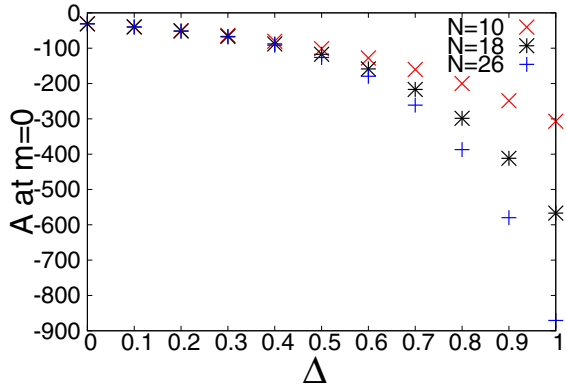

FIG. 8. Anisotropic parameter Δ dependence of the fourth derivative A at zero magnetization for several system sizes N: 10, 18, and 26. A appears to diverge for $\Delta > 1/2$ as the size dependence is large. Thus, the starting point of the anomaly of A is the $\Delta = 1/2$ point. The anomaly of A at $1/2 < \Delta < 1$ does not indicate the phase transition from the scaling dimension [10]. The $-1 < \Delta < 1/2$ region is named TL phase (I) and $1/2 < \Delta \leqslant 1$ is named TL phase (II) based on the behavior of A.

boundary is given by [32–34]

$$C(N, m) = \frac{b(m)}{N} - \frac{\pi v(m)}{24N^2}, \tag{44}$$

where $b(m)$ is a nonuniversal boundary term. In general, the convergence of this term is worse than that for a periodic boundary condition. We do not perform calculations for open boundary conditions herein, and leave them for future work.

Next, we discuss the correction term in two-dimensional systems. The correction term quickly converges, as shown by Nakano and Sakai [4], and thus, has convergence of at least second order. Unlike in the one-dimensional case, the convergence depends on the shape of the lattice. Figure 4 in Ref. [4] is different from Fig. 1(b) from the perspective of an energy gap, although it resembles Fig. 1(b) from previous research [4]. This problem will be addressed in our future works.

VI. ANOMALIES OF χ^{-1} AND A

In this section, we investigate the anomalies of χ^{-1} and A at zero and $m = 1/N$ for $0 \leqslant \Delta \leqslant 2$ from the perspective of size dependence. In addition, we reveal the anomalies of χ^{-1} and A. The origin of an anomaly is usually a phase transition or Neel state that indicates double degeneracy of ground states with an energy gap for the $S = 1/2$ XXZ chain.

First, the behaviors of χ and χ^{-1} are shown at zero magnetization in Fig. 9. Figure 9(a) shows that χ^{-1} becomes finite for $\Delta = 1$ in the thermodynamic limit. This indicates that the system does not have a finite spin gap or an anomaly. In contrast, Fig. 9(b) shows that χ^{-1} becomes infinite, i.e., χ reaches zero for $\Delta = 2$ in the thermodynamic limit. However, it is not conclusive that χ approaches zero in the thermodynamic limit. To solve this problem, we present Fig. 9(c), which is described as a semilog graph of Fig. 9(b). Figure 9(c) shows that the behavior of $\log \chi$ is consistent with the Ornstein-Zernike relation, which explains that $\ln \chi \propto -N/\xi + \ln N$, where ξ is the correlation length. Thus, χ for $\Delta = 2$ approaches zero, i.e., χ^{-1} approaches infinity in the thermodynamic limit. This indicates that the system has a finite spin gap and an anomaly for $\Delta = 2$. The origin of the anomaly is the Neel state. These facts are consistent with the results obtained by C. N. Yang and C. P. Yang [8,25]; thus, we observed an anomaly of the magnetic susceptibility in a one-dimensional system. Moreover, the observation of the anomaly is useful for distinguishing gapped from gapless systems.

Next, the behavior of A at zero magnetization is shown in Fig. 10. Figure 10(a) shows that A becomes finite for $\Delta = 0.3$ in the thermodynamic limit, whereas Fig. 10(b) shows that it is negative infinity for $\Delta = 0.7$ in the thermodynamic limit. For $\Delta = 0.7$, from Eq. (37), A is proportional to $N^{6-2x_T} = N^{0.6439}$, as the scaling dimension $x_T = 2.678003$ in Eq. (31). Thus, we plot the horizontal axis in Fig. 10(b) as $N^{-0.644}$. The behavior of A for $\Delta = 0.7$ is consistent with Eq. (37), in terms of both the power index and sign of the divergence. Both Figs. 10(c) and 10(d) show that A is negative infinity in the thermodynamic limit. For $\Delta = 1$, from Eq. (42), A is proportional to $N^{6-2x_T} = N^2$, as the scaling dimension $x_T = 2.0$. Thus, we plot the horizontal axis in Fig. 10(c) as N^{-2}. The behavior

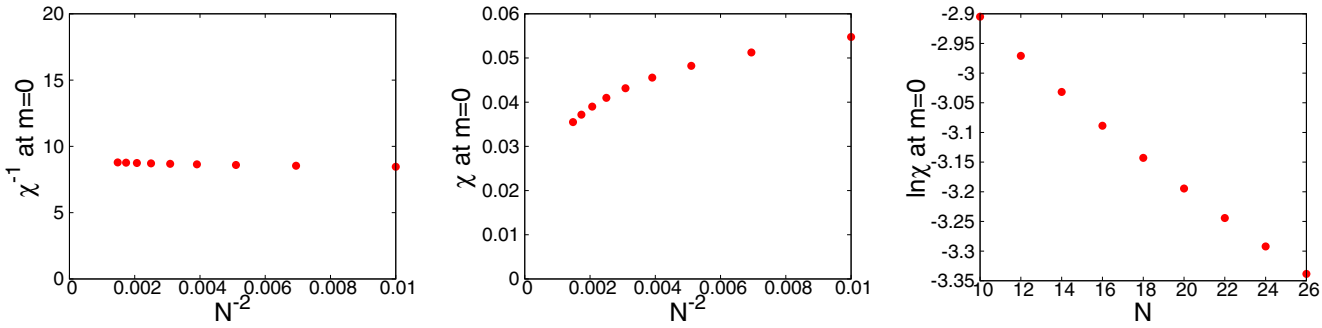

FIG. 9. N and N^{-2} dependence of the magnetic susceptibility χ and its inverse χ^{-1} at zero magnetization. Closed circles denote values of the magnetic susceptibility for several system sizes N: 10, 12, 14, 16, 18, 20, 22, 24, and 26. Panel (a) demonstrates that χ^{-1} becomes finite in the thermodynamic limit. Panel (c) demonstrates that $\log \chi$ approaches minus infinity in the thermodynamic limit because $\log \chi$ is consistent with the Ornstein-Zernike relation that explains $\ln \chi \propto -N/\xi + \ln N$, where ξ is the correlation length. Therefore, panel (b) demonstrates that χ approaches zero in the thermodynamic limit and shows an anomaly that indicates double degeneracy of ground states.

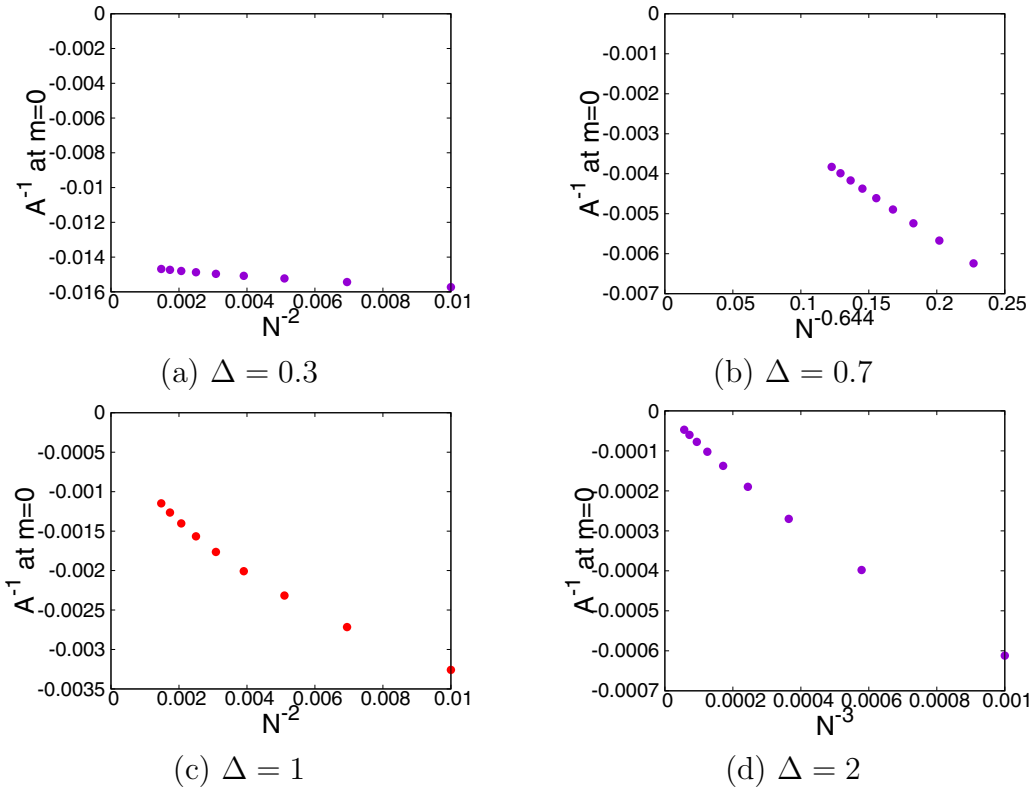

FIG. 10. N dependence of the fourth derivative A at zero magnetization. Closed circles denote values of A for several system sizes N: 10, 12, 14, 16, 18, 20, 22, 24, and 26. Panel (a) indicates that A becomes constant in the thermodynamic limit. Panel (b) indicates that A approaches minus infinity and is consistent with Eq. (37) in the thermodynamic limit. Both panels (c) and (d) demonstrate that A is minus infinity in the thermodynamic limit. These numerical data are consistent with Eqs. (42) and (16). Thus, these graphs show an anomaly that indicates Kosterlitz-Thouless (KT) transition for $\Delta = 1$ and double degeneracy of ground states for $\Delta = 2$.

of A for $\Delta = 1$ is consistent with Eq. (42), in terms of both the power index and sign of the divergence. For $\Delta = 2$, from Eq. (16), A is proportional to N^3. Therefore, we plot the horizontal axis in Fig. 10(d) as N^{-3}. The behavior of A for $\Delta = 2$ is consistent with Eq. (16), in terms of both the power index and sign of the divergence. These demonstrate that A shows an anomaly for $\Delta = 0.7, 1.0, 2.0$. However, the origin of the anomaly is different. For $\Delta = 0.7$, the origin is TL phase (II). The origin of the anomaly for $\Delta = 1$ is the phase transition, which means the transition from TL liquid phase to antiferromagnetic phase [8,9]. In contrast, in the $\Delta > 1$ region, a Neel state appears for the $S = 1/2$ XXZ chain. Thus, the origin of the anomaly for $\Delta = 2$ is the Neel state. Moreover, A shows the transition for $\Delta = 1$, although χ^{-1} does not show it from Fig. 9(a). The difference is used to confirm whether a phase transition happens or not. Therefore, observing A is helpful for determining the consistency of phase transition.

Finally, we show A at $m = 1/N$ in Fig. 11, as the behavior of A at $m = 1/N$ differs between Figs. 3(b) and 3(c). Figure 11(a) shows that A becomes finite for $\Delta = 0.3$ in the thermodynamic limit, whereas Fig. 10(b) shows that it is minus infinity for $\Delta = 0.7$ in the thermodynamic limit. The behavior of A for $\Delta = 0.7$ is consistent with Eq. (35). The origin of the anomaly is TL phase (II). It appears that A in Fig. 11(c) becomes finite for $\Delta = 1$. However, the behavior of A is not consistent with Eq. (40), in which A reaches infinity when m approaches zero. The disagreement results from the intermediate region in Eq. (40), in which A exhibits flat and negative behavior, before reaching a sufficiently small region $|m| \ll 1$. Thus, A becomes infinite as the system size becomes larger in our calculation. The origin of the anomaly is phase transition. In contrast, Fig. 11(d) shows that A reaches infinity for $\Delta = 2$ in the thermodynamic limit. The behavior of A is consistent with Eq. (16). This indicates that A shows an anomaly for $\Delta = 2$. The origin of the anomaly is a Neel state. Therefore, the behavior of A at $m = 1/N$ in Figs. 3(b) and 3(c) is explained by Eqs. (16) and (40). Observation of the change in behavior at $m = 1/N$ can be proposed as a new technique to distinguish gapped from gapless systems. Hence, observing A at $m = 1/N$ allows us to distinguish gapped from gapless systems. However, future works must focus on the exact solutions of A at $m = 1/N$, as few investigations have focused on this behavior.

These findings indicate that observation of A is more efficient than that of χ. Thus, we expect this technique to be used for analysis of spin liquids with spin gap issues in triangular and Kagome lattices [4–7].

VII. CONCLUSION

We investigated anomalies of χ and A for the $S = 1/2$ XXZ antiferromagnetic chain by numerical diagonalization. At zero magnetization, χ^{-1} shows an anomaly for $\Delta > 1$. At zero magnetization, A clearly indicates an anomaly for

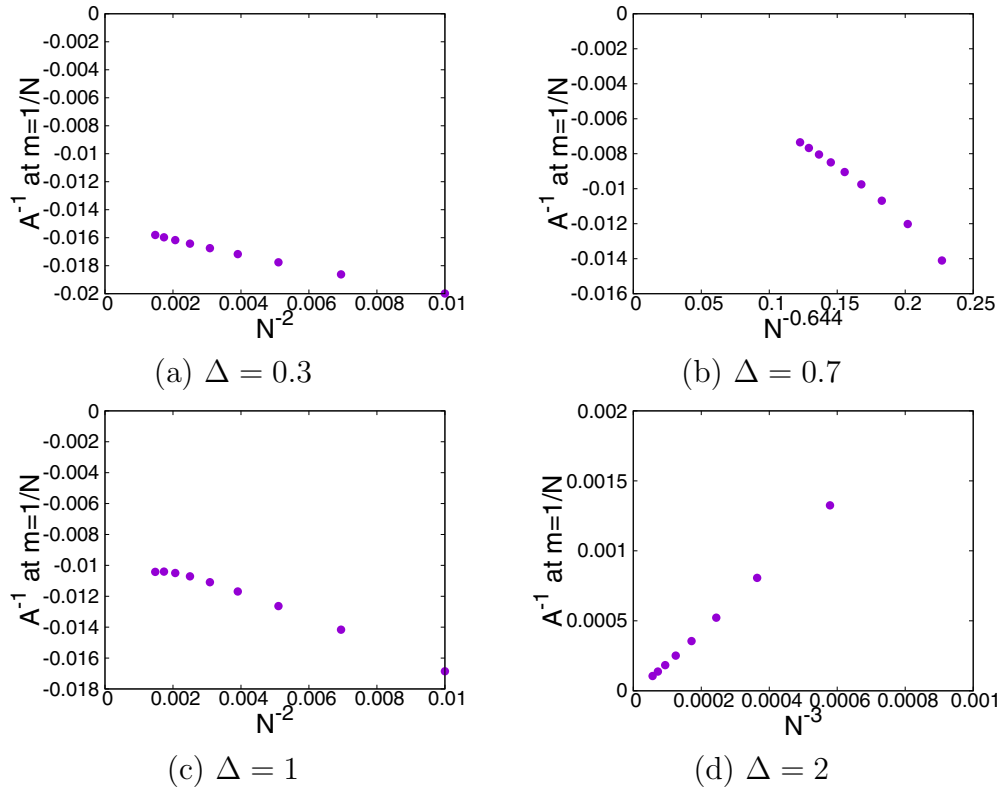

FIG. 11. N dependence of the fourth derivative A^{-1} at $m = 1/N$. Closed circles denote values of A for several system sizes N: 10, 12, 14, 16, 18, 20, 22, 24, and 26. Panel (a) indicates that A becomes finite in the thermodynamic limit. Panel (b) indicates that A approaches minus infinity and is consistent with Eq. (35) in the thermodynamic limit. Panel (c) appears to indicate that A becomes finite. However, it disagrees with Eq. (40), in which A approaches infinity as the magnetization approaches zero. The disagreement results from the intermediate region in Eq. (40), in which A exhibits a negative and flat region. Thus, A approaches infinity as the system size becomes larger. Panel (d) demonstrates that A is infinity and is consistent with Eq. (16) in the thermodynamic limit. Thus, panel (d) shows an anomaly that indicates double degeneracy of ground states.

$\Delta > 1/2$. In addition, an anomaly of A at $m = 1/N$ is shown for $\Delta > 1$. In contrast, in the $\Delta < 0$ region, future works are required regarding the anomalies of χ and A in numerical calculations. The results indicate that χ and A have anomalies, and that observing the anomaly of A is easier than that of χ for relatively small system sizes. In other words, the observation of phase transition is easier by A than by χ. We reveal that the TL phase can be divided into $-1 < \Delta < 1/2$ as TL phase (I) and $1/2 < \Delta \leqslant 1$ as TL phase (II), from the perspective of the anomaly of A at $\Delta = 1/2$. Therefore, we conclude that observation of A is a useful method of analyzing critical phenomena, compared to that of χ.

Our study is concerned with one-dimensional systems. However, our method can be used regardless of dimensions. This method will help investigate quantum spin systems in two or three dimensions. In addition, this method can be applied to other systems such as spin liquids. The behavior of spin liquids has been studied for magnetic susceptibility [4,7] and our method using A, compared to that using χ, will be useful for researching the behavior of a spin liquid that has spin gap issues. The study of using A for other models and higher dimension is left for future works.

In particular, A relates to the nonlinear magnetic susceptibility [35] of quantum spin systems and is thus of direct relevance to experiments. The nonlinear magnetic susceptibility can be easily calculated with high accuracy using A. The method using A can be a new technique in the study of quantum spin systems and strongly correlated electron systems. Furthermore, the method will enable one to discover a magnetization plateau observed in experiments that shows constant magnetization when a magnetic field changes. The plateau indicates the anomaly of χ, and that of A should also appear there from Eqs. (15) and (16). The observations of χ and A will be useful for evaluating a magnetization plateau. Numerical diagonalization calculations of A will provide us with a new development in theory and experiments for quantum spin systems.

ACKNOWLEDGMENTS

We would like to thank Professors T. Sakai, M. Takahashi, T. Matsui, and J. Fukuda for their helpful discussions. We would like to thank Editage [36] for English language editing. Our calculations on numerical diagonalization were performed using TITPACK Version 2, which Prof. H. Nishimori coded, and $H\phi$, which Prof. M. Kawamura *et al.* coded.

[1] H. A. Bethe, Z. Phys. **71**, 205 (1931).
[2] F. D. M. Haldane, Phys. Rev. Lett. **50**, 1153 (1983).
[3] J. des Cloizeaux and M. Gaudin, J. Math. Phys. **7**, 1384 (1966).
[4] H. Nakano and T. Sakai, J. Phys.: Conf. Ser. **868**, 012006 (2017).
[5] H. Nakano and T. Sakai, J. Phys. Soc. Jpn. **80**, 053704 (2011).
[6] T. Sakai and H. Nakano, Physica B **536**, 85 (2018).
[7] T. Sakai and H. Nakano, J. Phys.: Conf. Ser. **969**, 012127 (2018).
[8] C. N. Yang and C. P. Yang, Phys. Rev. **151**, 258 (1966).
[9] M. Takahashi, *Thermodynamics of One-Dimensional Solvable Models* (Cambridge University Press, Cambridge, England, 1999), pp. 54–56.
[10] J. Cardy, *Scaling and Renormalization in Statistical Physics* (Cambridge University Press, Cambridge, England, 1996).
[11] P. Ginsparg, Applied conformal field theory, in *Fields, Strings and Critical Phenomena*, Les Houches, Session XLIX, 1988, edited by E. Brézin and J. Zinn-Justin (North-Holland, Amsterdam, 1989).
[12] S. K. Yang, Nucl. Phys. B **285**, 183 (1987).
[13] T. Sakai and M. Takahashi, Phys. Rev. B **43**, 13383 (1991).
[14] H. Nishimori, http://hdl.handle.net/2433/94584 (1991).
[15] M. Kawamura, K. Yoshimi, T. Misawa, Y. Yamaji, S. Todo, and N. Kawashima, Comput. Phys. Commun. **217**, 180 (2017).
[16] N. Goldenfeld, *Lectures on Phase Transition and the Renormalization Group* (Westview Press, Boulder, 1992).
[17] L. Faddeev, in *Développments Récents en Théorie des champs et Mécanique Statistique*, edited by R. Stora and J. Zuber (North-Holland, Amsterdam, 1983).
[18] E. Lieb, T. Schultz, and D. Mattis, Ann. Phys. (NY) **16**, 407 (1961).
[19] K. Nomura, Phys. Rev. B **48**, 16814 (1993).
[20] I. Affleck and E. H. Lieb, Lett. Math. Phys. **12**, 57 (1986).
[21] M. Takahashi and T. Sakai, J. Phys. Soc. Jpn. **60**, 760 (1991).
[22] K. Kawano and M. Takahashi, J. Phys. Soc. Jpn. **64**, 4331 (1995).
[23] R. B. Griffiths, Phys. Rev. **133**, A768 (1964).
[24] S. Eggert, I. Affleck, and M. Takahashi, Phys. Rev. Lett. **73**, 332 (1994).
[25] C. N. Yang and C. P. Yang, Phys. Rev. **150**, 327 (1966).
[26] J. Cardy, "Conformal invariance," in *Phase Transitions*, edited by C. Domb and J. L. Lebowitz, Vol. 11 (Academic, New York, 1987).
[27] K. Nomura, J. Phys. A: Math. Gen **28**, 5451 (1995).
[28] A. Luther and I. Peschel, Phys. Rev. B **12**, 3908 (1975).
[29] A. W. W. Ludwig, J. L. Cardy, Nucl. Phys. B **285**, 687 (1987).
[30] A. Kitazawa and K. Nomura, J. Phys. Soc. Jpn. **66**, 3944 (1997).
[31] L. P. Kadanoff, Ann. Phys. (NY) **120**, 39 (1979).
[32] H. W. J. Blöte, J. L. Cardy, and M. P. Nightingale, Phys. Rev. Lett. **56**, 742 (1986).
[33] I. Affleck, Phys. Rev. Lett. **56**, 746 (1986).
[34] J. L. Cardy, J. Phys. A **17**, L385 (1984).
[35] M. Suzuki, Prog. Theor. Phys. **58**, 1151 (1977).
[36] www.editage.com.